# MAT 280: Laplacian Eigenfunctions: Theory, Applications, and Computations
# Lectures 14: Shape Recognition Using Laplacian Eigenvalues and Computational Methods of Laplacian Eigenvalues/Eigenfunctions

Lecturer: Naoki Saito
Scribe: Zhihua Zhang / Allen Xue

May 15 & 17 , 2007

## 1 Shape recognition using Laplacian eigenvalues

In this section, we will introduce the work of Kbabou, Hermi, and Rhonma (2007)[2]. Their main idea is to use the eigenvalues and their ratios of the Dirichlet-Laplacian for various planar shapes as their features for classifying them.

### 1.1 Recall some special geometric inequalities (2D)

Let the sequence $0 < \lambda_1 < \lambda_2 \leq \lambda_3 \leq \cdots \leq \lambda_k \leq \cdots \to \infty$ be the sequence of eigenvalues of Dirichlet-Laplacian problem: $-\Delta u = \lambda u$ in a given bounded planar domain $\Omega$ with Dirichlet boundary condition $u = 0$ on its boundary $\partial\Omega$.

### 1.1.1 Universal Inequalities

- Payne-Pólya-Weinberger inequalities [7].

$$\begin{cases} \lambda_{m+1} - \lambda_m \leq 2 \cdot \dfrac{1}{m} \sum_{j=1}^{m} \lambda_j, \\ \\ \dfrac{\lambda_{m+1}}{\lambda_m} \leq 3. \end{cases}$$

- Hile-Protter inequality [8].

$$\sum_{j=1}^{m} \frac{\lambda_j}{\lambda_{m+1} - \lambda_j} \geq \frac{m}{2}.$$

- Yang inequalities [9].

$$\begin{cases} \sum_{j=1}^{m} (\lambda_{m+1} - \lambda_j)^2 \leq 2 \sum_{j=1}^{m} \lambda_j (\lambda_{m+1} - \lambda_j), \\ \\ \lambda_{m+1} \leq 3 \cdot \dfrac{1}{m} \sum_{j=1}^{m} \lambda_j. \end{cases}$$

### 1.1.2 Isoperimetric inequalities

- Faber-Krahn inequality [10].

$$\lambda_1 \geq \frac{\pi^2 j_{0,1}^2}{|\Omega|^2},$$

- Ashbaugh-Benguria inequality [11].

$$\frac{\lambda_2}{\lambda_1} \leq \frac{j_{1,1}^2}{j_{0,1}^2} \approx 2.5387,$$

where $j_{0,1} \approx 2.4048$ and $j_{1,1} \approx 3.83171$ are the first positive zeros of the Bessel functions $J_0(x)$ and $J_1(x)$, respectively. And $|\Omega|$ is the area of $\Omega$. The equalities are attained in the above two formulas if and only if the domain $\Omega$ is a $2D$ disk.

### 1.1.3 Other Properties

**(a) Domain monotonicity property** As we have shown in the previous lecture, if $\Omega_1 \subset \Omega_2$, then

$$\lambda_k(\Omega_1) \geq \lambda_k(\Omega_2), \qquad k \in \mathbb{N}.$$

**(b) Scaling Property: (see [1], [3])**

$$\lambda_k(\alpha\,\Omega) = \frac{\lambda_k(\Omega)}{\alpha^2} \qquad \forall\ \alpha > 0,\ \ k \in \mathbb{N}.$$

where $\alpha\Omega$ is a scaling by factor $\alpha$ of $\Omega$. This implies

$$\frac{\lambda_k(\alpha\,\Omega)}{\lambda_m(\alpha\,\Omega)} = \frac{\lambda_k(\Omega)}{\lambda_m(\Omega)} \qquad \forall\ k,\ m \in \mathbb{N}.$$

From this, we see that the ratios of Laplacian eigenvalues are *scale invariant*.

**(c) Laplacian eigenvalues are translation and rotation invariant.**

## 1.2 Features used by Khabou, Hermi, and Rhouma

Let $\Omega$ be a domain represented by a binary image. Using the Dirichlet-Laplacian eigenvalues for $\Omega$, define three sets of features as follows.

$$F_1(\Omega) \triangleq \left\{ \left( \frac{\lambda_1}{\lambda_2}, \quad \frac{\lambda_1}{\lambda_3}, \quad \ldots, \quad \frac{\lambda_1}{\lambda_n} \right) \right\},$$

$$F_2(\Omega) \triangleq \left\{ \left( \frac{\lambda_1}{\lambda_2}, \quad \frac{\lambda_2}{\lambda_3}, \quad \ldots, \quad \frac{\lambda_{n-1}}{\lambda_n} \right) \right\},$$

$$F_3(\Omega) \triangleq \left\{ \left( \frac{\lambda_1}{\lambda_2} - \frac{d_1}{d_2}, \quad \frac{\lambda_1}{\lambda_3} - \frac{d_1}{d_3}, \quad \ldots, \quad \frac{\lambda_1}{\lambda_n} - \frac{d_1}{d_n} \right) \right\},$$

where $0 < d_1 < d_2 = d_3 < d_4 = d_5 < \cdots \leq d_n$ are the Dirichlet-Laplacian (D-L) eigenvalues for the unit disk in $2D$.

First of all, we can get

$$0 < F_j(\Omega)_\ell \leq 1, \quad j = 1, 2, \qquad |F_3(\Omega)_\ell| \leq 1,$$

where $F_j(\Omega)_\ell$ is the $\ell$th component of each vector in $F_j(\Omega)$.

It is interesting to consider that $F_3$ measures the deviation of $\Omega$ from the 2D disk (not necessarily unit disk). The optimal $n$ depends on the problem being addressed. Khabou, Hermi, and Rhouma have shown that the three sets of features were tolerant of boundary noise and deformation and have good inter-class discrimination capabilities. The three sets of features were used successfully to classify natural and man-made images with a high degree of accuracy and using a relatively small number of features. Reuter, Wolter, and Peinecke [3] introduces a method to extract "Shape-DNA", a numerical fingerprint or signature, of any 2D or 3D manifold (surface or solid) by taking the eigenvalues (i.e., the spectrum) of its Laplace-Beltrami operator. Since the spectrum is an isometry invariant, it is independent of the object's representation including parametrization and spatial position. Additionally, the eigenvalues can be normalized so that uniform scaling factor for the geometric objects can be obtained easily.

# 2 Computational Method of Laplacian Eigenvalues

In this section, we will discuss three methods to compute Laplacian eigenvalues and eigenvectors..

## 2.1 Finite Difference Scheme [2].

Its main idea is to discretize the equation $-\Delta u = \lambda u$ by the finite difference approximation

$$-\frac{1}{h^2}\left[\ u_{i+1,j} + u_{i,j+1} + u_{i-1,j} + u_{i,j-1} - 4u_{ij}\ \right] = \lambda u_{ij}.$$

Here the domain $\Omega$ is cut into squares of side $h$, $u_{ij}$ is the value of the eigenfunction corresponding to $\lambda$ at the lattice point $(ih, jh)$. The convergence rate of this method is $O(h^2)$. Moreover, it is slow and inaccurate for $\Omega$ of a complicated shape with a large number of grid points.

## 2.2 Finite Element Method [3].

Many people use this in practice. It is better for general $\Omega$. But it is still very cumbersome. Here we just briefly describe the idea of finite element method.

From Equation $-\Delta u = \lambda u$, it follows that for any trial function $\varphi$ with $\varphi = 0$ on the boundary of $\Omega$,

$$-\iint_\Omega \varphi\, \Delta u \,\mathrm{d}\boldsymbol{x} = \lambda \iint_\Omega \varphi\, u \,\mathrm{d}\boldsymbol{x}.$$

By Green's first identity, $-\iint_\Omega \varphi \Delta u \,\mathrm{d}\boldsymbol{x} = \iint_\Omega \nabla\varphi \cdot \nabla u \,\mathrm{d}\boldsymbol{x}$. This implies that

$$\iint_\Omega \nabla\varphi \cdot \nabla u \,\mathrm{d}\boldsymbol{x} = \lambda \iint_\Omega \varphi\, u \,\mathrm{d}\boldsymbol{x}. \tag{1}$$

We choose $n$ linearly independent functions $F_1, ..., F_n$ which are the linear, quadratic or cubic polynomials on every tetrahedral element of $\Omega$ and satisfy $F_k = 0$ on the boundary of $\Omega$. Take their linear combination as approximation of the solution $u$, i.e.,

$$u \approx \sum_{i=1}^{n} U_i\, F_i, \quad U_i \in \mathbb{R}. \tag{2}$$

Again, let $\varphi = F_k$. So

$$\iint_\Omega \nabla\varphi \cdot \nabla u \,\mathrm{d}\boldsymbol{x} = \sum_{i=1}^{n} a_{ki}\, U_i, \qquad k = 1, ..., n,$$

where

$$a_{ki} = \iint_\Omega \sum_{j=1}^{n} \left(\frac{\partial F_k}{\partial x_j}\right) \left(\frac{\partial F_i}{\partial x_j}\right) \mathrm{d}\boldsymbol{x}.$$

On the other hand,

$$\iint_\Omega \varphi\, u \,\mathrm{d}\boldsymbol{x} = \sum_{i=1}^{n} b_{ki}\, U_i, \quad k = 1, ..., n,$$

where

$$b_{ki} = \iint_\Omega F_k\, F_i \,\mathrm{d}\boldsymbol{x}.$$

From this and (1), one obtains that

$$\sum_{i=1}^{n} a_{ki}\, U_i = \lambda \sum_{i=1}^{n} b_{ki}\, U_i, \quad k = 1, ..., n.$$

Define the matrix $A = (a_{ki})$ and $B = (b_{ki})$. Then (1) can be written as

$$A\boldsymbol{U} = \lambda B\boldsymbol{U}, \quad \text{where} \quad \boldsymbol{U} = (U_1, ..., U_n)^T.$$

So $\lambda$ and $\boldsymbol{U}$ can be calculated. Furthermore, the eigenfunction $u$ is obtained by (2).

## 2.3 Method of Particular Solutions (MPS) [4], [5].

### 2.3.1 History of MPS

In 1967, Fox, Henrici, and Moler (FHM) [5] described the MPS. The famous example was the Dirichlet-Laplacian eigenfunctions of a $L-$shaped region, which turns be the logo of MATLAB. Note that the actual MATLAB logo fails to satisfy the Dirichlet boundary condition, which was intentionally done for visual purpose.

Since the MPS runs into difficulties when dealing with more complicated regions, after the early 1970s, the MPS got less attention. Later on, Descloux and Tolley presented other method based on local expansions near each vertex [6]. Betcke and Trefethen proposed a modification of MPS [4]. The crucial changes are to work not only with boundary points, but also interior points of the domain. The modified MPS can deal with quite complicated domains.

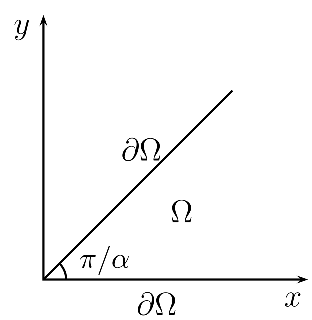


Figure 1: An unbounded domain $\Omega$ with interior angle of the wedge.

### 2.3.2 The Dirichlet-Laplacian problem in an unbounded wedge

As shown in Figure 1, if the interior angle of the wedge is $\frac{\pi}{\alpha}$, then we have the D-L eigenfunctions

$$\varphi(r,\theta) = J_{\alpha k}(\sqrt{\lambda}\ r)\sin\alpha k\theta, \quad k \in N \setminus \{0\}$$

for any $\lambda > 0$, where $J_{\alpha k}$ is a Bessel function of the first kind with order $\alpha k$. The spectrum is continuous.

In general, the Dirichlet-Laplacian eigenfunctions are in $C^{\infty}(\Omega) \bigcup C(\overline{\Omega})$. If there exists a corner in $\partial\Omega$ with angle $\frac{\pi}{k},\;\; k \in \mathbb{N}$, then we can do odd (even for the Neumann-Laplacian problem) reflection $k-1$ times followed by one reflection to get a continuous extension of the eigenfunction $\varphi$ in the whole neighborhood of the corner. Such a corner is called *regular* corner; otherwise, i.e., $\frac{\pi}{\alpha}$, $\alpha \in \mathbb{R}_+ \backslash \mathbb{N}$, is called *singular*. For a singular corner, it is not possible to extend the eigenfunction analytically to a whole neighborhood of that corner.

### 2.3.3 The Original Method of Particular Solutions (MPS)

Its main idea is as follows.

(1) Consider various solutions of $-\Delta u = \lambda u$ in $\Omega$ for a given value of $\lambda$. They are called *particular solutions*.

(2) Try to vary $\lambda$ until we can find a linear combination of such solutions that satisfies the Dirichlet boundary condition $u = 0$ on $\partial\Omega$, at a number of sample points of $\partial\Omega$.

**Example 2.1.** A convenient set of particular solutions near a corner of angle $\frac{\pi}{\alpha}$ are

$$\left\{ \varphi^{(k)}(r,\,\theta) = J_{\alpha k}(\sqrt{\lambda}\; r)\sin(\alpha k\theta) \right\}_{k\in\mathbb{N}}.$$

We call these the *Fourier-Bessel* functions. These functions happen to satisfy the Dirichlet boundary condition along the line segments.

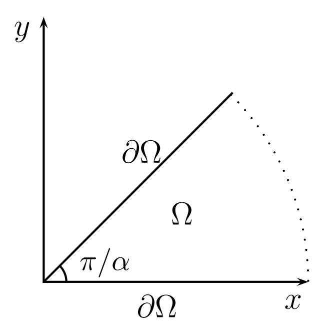


Figure 2: A bounded domain $\Omega$ with interior angle of the wedge.

Consider an approximate eigenfunction

$$\varphi^*(r,\ \theta) = \sum_{k=1}^{N} c_k^{(N)} \varphi^{(k)}(r,\ \theta),$$

with $c_k^{(N)}$ to be determined so as to satisfy the Dirichlet boundary condition on the remainder of the boundary (e.g., the dotted line part in Figure 2).

One approach is to set the collocation points, i.e., sampling points, on the boundary $(r_i,\ \theta_i),\ \ i = 1, ..., N$ such that

$$\varphi^*(r_i,\ \theta_i) = 0, \quad \forall i = 1, \ldots, N.$$

This leads to a nonlinear system of equations

$$A(\lambda)\boldsymbol{c} = \mathbf{0},$$

where

$$\boldsymbol{c} = (c_1^{(N)},\ ...,\ c_N^{(N)})^T \in \mathbb{R}^N,$$
$$A(\lambda) = (\ a_{jk}(\lambda)\ ) \in \mathbb{R}^{N\times N},$$
$$a_{jk}(\lambda) \triangleq J_{\alpha k}(\sqrt{\lambda}\ r_j) \sin(\alpha k\, \theta_j), \quad j, k = 1, \ldots, N.$$

The FHM approach [5] is to look for a zero of $\det A(\lambda)$, and then solve for $\boldsymbol{c}$ (modulo constant multiplications).

An alternative approach proposed by Moler (1969) is to choose $M$ $(M > N)$ samples on the boundary. Then $A(\lambda) \in \mathbb{R}^{M\times N}$. Again, look for a zero or near zero of *the smallest singular value* of $A(\lambda)$. This was superior to the original FHM method.

Unfortunately, the FHM method fails to obtain more than four digits of accuracy, the method breaks down after $N = 14$ per remaining edge of the boundary of the L-shaped region.

### 2.3.4 Failure of the MPS

The aim of the MPS is to find a value $\lambda$ such that there exists a nontrivial linear combination of the Fourier-Bessel functions that is 0 at the collocation points on $\partial\Omega$. If $\lambda$ is not close to an actual eigenvalue, then we expect

$$A(\lambda)\boldsymbol{c} = \mathbf{0}$$

to have no nontrivial solution. The problem is that Fourier-Bessel functions behave similarly to a power basis $z^k$ and the condition number of $A(\lambda)$ grows exponentially as $N$ increases. This also happens for any value of $\lambda$, whether or not it is an eigenvalue. Consequently, when $N$ is large, it is always possible to find a linear combination of columns of $A(\lambda)$ that are close to zero. If $\lambda$ is not close to an eigenvalue, this results in approximating the zero function which is not a D-L eigenfunction. Since the MPS method examines only boundary points, it cannot distinguish zero functions and the D-L eigenfunction.

### 2.3.5 A modified method

The idea of Betcke and Trefethen is to impose constraints using some interior points from $\Omega$ (see Figure 3). Let

$$\begin{aligned} m_B &\triangleq \# \text{ of boundary collocation points}, \\ m_I &\triangleq \# \text{ of interior collocation points}, \\ m &\triangleq m_B + m_I. \end{aligned}$$

Let $\boldsymbol{\varphi} \in \mathbb{R}^m$ be a vector containing the values of eigenfunction $\varphi(r,\ \theta)$ at these $m$ points. We order the entries of $\boldsymbol{\varphi}$ such that the first $m_B$ entries correspond to the boundary collocation points and the remaining $m_I$ entries correspond to the interior collocation points. Now the matrix $A(\lambda)$ has more rows:

$$A(\lambda) = \begin{bmatrix} A_B(\lambda) \\ \\ A_I(\lambda) \end{bmatrix} \in \mathbb{R}^{m\times N}$$

with $B$ and $I$ corresponding to boundary and interior. Let $\mathcal{A}(\lambda)$ be the space of trial functions sampled at boundary and interior points, i.e.,

$$\mathcal{A}(\lambda) \triangleq \text{range } (A(\lambda)) \subset \mathbb{R}^m.$$

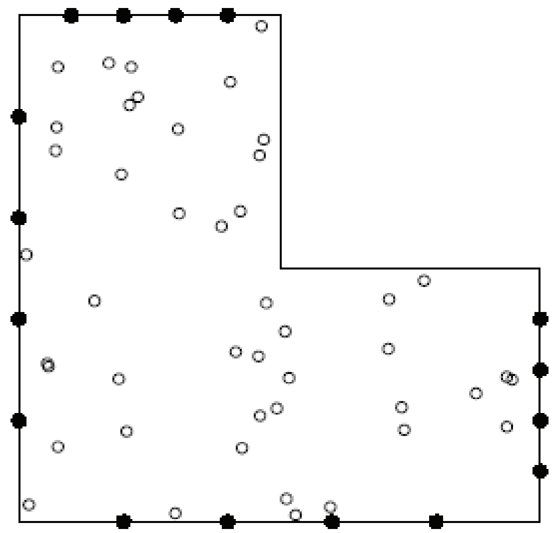

Figure 3: In the modified method, the Fourier-Bessel functions are sampled at interior as well as boundary points. The interior points are chosen randomly.

Construct an orthonormal basis of $\mathcal{A}(\lambda)$ via QR factorization of $A(\lambda)$. Set

$$Q(\lambda) = \begin{bmatrix} Q_B(\lambda) \\ \\ Q_I(\lambda) \end{bmatrix} \in \mathbb{R}^{m \times N}.$$

Now, for $\boldsymbol{\varphi} \in \mathcal{A}(\lambda), \ \| \boldsymbol{\varphi} \| = 1$, there exists a vector $\boldsymbol{\psi} \in \mathbb{R}^N$ such that

$$\boldsymbol{\varphi} = Q(\lambda)\boldsymbol{\psi},$$

$$\| \boldsymbol{\psi} \| = 1.$$

Because $Q(\lambda)$ is orthonormal,

$$Q^T(\lambda)\, Q(\lambda) = I_N, \quad \text{if } m > N.$$

Consider the minimization problem

$$\min_{\boldsymbol{\psi} \in \mathbb{R}^N, \ \|\boldsymbol{\psi}\|=1} \| \, Q_B(\lambda)\boldsymbol{\psi} \, \|, \tag{1}$$

which is exactly to minimize the boundary part of $\boldsymbol{\varphi}$. The minimizer of (1) is the right singular vector of $Q(\lambda)$ corresponding to the smallest singular value of $Q_B(\lambda)$. Let this singular value be denoted by $\sigma_B(\lambda)$ and the minimizer by $\widetilde{\boldsymbol{\psi}}$. Then

$$\sigma_B(\lambda) = \min_{\boldsymbol{\psi}\in\mathbb{R}^N,\ \|\boldsymbol{\psi}\|=1} \| Q_B(\lambda)\boldsymbol{\psi} \| = \| Q_B(\lambda)\widetilde{\boldsymbol{\psi}} \| .$$

Let $\widetilde{\boldsymbol{\varphi}} = Q(\lambda)\widetilde{\boldsymbol{\psi}}$. Then

$$1 = \| \widetilde{\boldsymbol{\varphi}} \|^2 = \left\| \begin{bmatrix} Q_B(\lambda) \\ Q_I(\lambda) \end{bmatrix} \widetilde{\boldsymbol{\psi}} \right\|^2 = \sigma_B^2(\lambda) + \| Q_I(\lambda)\widetilde{\boldsymbol{\psi}} \|^2 .$$

Here $\sigma_B(\lambda) \approx 0$ and $\| Q_I(\lambda)\widetilde{\boldsymbol{\psi}} \| \approx 1$.

So, at the interior points, $\widetilde{\boldsymbol{\varphi}}$ are not zeros automatically. Using this method, Betcke and Trefether could compute the D-L eigenvalues with 14 digits accuracy.

# References


[1] R. Courant, D. Hilbert, *Methods of Mathematical Physics*, Vol. I, Wiley-Interscience, 1953.

[2] M. A. Khabou, L. Hermi, M. B. H. Rhouma: Shape Recognition Using Eigenvalues of the Dirichlet Laplacian, *Pattern Recognition*, vol. 40, pp. 141–153, 2007.

[3] M. Reuter, F. E. Wolter, N. Peinecke: Laplace-Beltrami Spectra as Shape-DNA of Surfaces and Solids, *Computer-Aided Design*, vol. 38, pp. 342–366, 2006.

[4] T. Betcke, L. N. Trefethen: Reviving the Method of Particular Solutions, *SIAM Review*, vol. 47, no. 3, pp. 469–491, 2005.

[5] L. Fox, P. Henrici, C. Moler: Approximations and Bounds for Eigenvalues of Elliptic Operators, *SIAM J. Numer. Anal.* vol. 4, no. 1, pp. 89–102,1967.

[6] J. Descloux, M. Tolley: An accurate algorithm for computing the eigenvalues of a polygonal membrane, *Comput. Methods Appl. Mech. Engrg.*, vol. 39, pp. 37–53, 1983.

[7] L. E. PAYNE, G. PÓLYA, H. F. WEINBERGER: On the ratio of consecutive eigenvalues, *J. Math. Phys.*, vol. 35, pp. 289–298, 1956.

[8] G. N. HILE, M. H. PROTTER: Inequalities for eigenvalues of the Laplacian, *Indiana Univ. Math. J.*, vol. 29, pp. 523–538, 1980.

[9] H. C. YANG: Estimate of the difference between consecutive eigenvalues, 1995 preprint (revision of International Centre for Theoretical Physics preprint IC/91/60, Trieste, Italy, April 1991).

[10] I. CHAVEL: Eigenvalues in Riemannian Geometry, *Academic Press*, New York, 1984.

[11] M. S. ASHBAUGH: The universal eigenvalue bounds of Payne-Pólya-Weinberger, Hile-Protter, and H.C. Yang, in: Spectral and inverse spectral theory, *Proc. Indian Acad. Sci. Math. Sci.*, vol. 112, pp. 3–30, 2002.